

## NANOSTRUCTURED POROUS SILICON: PROPERTIES MODIFICATION

**L. Monastyrskii**

Department of Physics, Iv. Franko Lviv State University,  
50 Dragomanov str., Lviv, UKRAINE

### INTRODUCTION

At present time the porous silicon is a perspective material for microelectronics as a high resistivity material.

In 1990, Cauham [1] in Appl. Phys. Letters for the first time reported about exotic visible room-temperature photoluminescence of porous silicon. So it become possible to create light-emitting diodes (LED) and lasers on the same substrate of Si. Porous silicon may be a new material for integrated micro- and optoelectronics.

### EXPERIMENTAL METHODS

Layers of porous silicon (PS) were obtained by electrochemical etching of n,p-types monocrystalline silicon in HF-ethanolic solution. We used (111) Si substrates with thickness of about 400  $\mu\text{m}$ . HF-ethanolic solution with 25% HF concentration was used as the electrolyte. Specimens of n-type conductivity were irradiated by white light during electrochemical etching. After anodization, some specimens were etched in concentrated HF about 2.5 h for increasing the porosity [1].

Studies of surface and near surface region of por-Si were done by ellipsometry on wavelength of He-Ne laser (633 nm). As a result of the experiment we have obtained polarization angles  $\psi$  and  $\Delta$  for different angles of incident light. Using the measured values, the inverse problem of ellipsometry – determination of refractive index  $n$ , absorption coefficient  $k$ , layers thickness  $d$  – has been solved. It was necessary to use two- or three-layers model and to create computer programme for obtaining  $n$ ,  $k$ ,

d values of por-Si layers. We also investigated the influence of technological conditions on optical constants of por-Si and porosity  $p$  of the material. The porosity was calculated on the base of  $n$  and  $k$  using Lorentz-Lorenz equation [2]. Error of calculations was about 10%.

The Thermo Stimulated Depolarisation Current (TSDC) investigation was made by formed thermoelectret state in the sample PS with area  $1 \text{ cm}^2$  in vacuum cryostat. Polarisation was carried out in the electric field of the capacitor cell at the temperature between 450 and 480 K. The electric field was of *ca.*  $1 \cdot 2 \cdot 10^4 \text{ V/m}$ . After switching off the polarising electric field, the TSD current has been measured with linear heating [3].

In order to identify the nature of the defects responsible for the electret state, we have carried out the analysis of the energy distribution  $g(E)$  of the energy involved in polarization defect. We have calculated  $g(E)$  [3] by numerical solving of the Fredholm integral equation (which is based on the Tikhonov's regularisation method), according to the phenomenological theory of TSD current for disordered dielectric.

We have investigated paramagnetic properties of PS after heat treatment in vacuum under high temperature (up to 625 K). Spin centres spectra were recorded using an RADIOPAN SE/X-2544 and RE-1306 commercial rf spectrometers, operating in the high-frequency (100 kHz) modulation mode of magnetic field at temperatures 300 K and 77 K.

The effective  $g$ -factor values of paramagnetic centres were defined from the experimental spectra using  $h\nu = g_{\text{eff}}\beta H$  relationship, where  $H$  is the resonance magnetic field,  $\nu$  is the microwave frequency,  $h$  is Planck's constant, and  $\beta$  is Bohr magneton. The microwave frequency in each case was controlled by means of the DPPH frequency marker ( $g = 2.0036 \pm 0.0002$ ).

The photoluminescence (PL) and electroluminescence (EL) in visible (400–800 nm) spectrum range was studied by automatic

equipment. Exciting of luminescence was obtained by nitrogen or argon lasers with wavelength 337 and 488 nm, respectively. The Auger Electron Spectroscopy (AES) measurements of  $dN(E)/dE$  derivative amplitudes were carried out with cylindrical mirror analyzer resolution 0.5% and 3 keV primary beam energy in vacuum  $10^{-7}$  Pa. Thermo Stimulated Exoelectron Emission (TSEE) spectra were recorded in 295-650 K range with heating rate  $\beta = 0.15$  K/s at pulse counts per second (cps) regime.

PS EL was recorded by us in electrochemical cell with 0.5M  $H_2SO_4 + 0.1M K_2S_2O_8$  electrolyte in current injection regime. Initial PS layers were created on n-Si (100) substrates with resistivity  $4.5 \Omega \cdot cm$  by anode etching in HF ethanol solution with current density  $10 \text{ mA}/cm^2$  and white light irradiation during 30 seconds. Direct or pulsed current of various duration and polarity in the current stabilization regime was applied between ohmic contact to the silicon substrate and platinum electrode. Cathodoluminescence (CL) of PS was studied in 300-700 nm spectrum range. The electron beam exiting had the following parameters:  $U=9 \text{ KV}$ ,  $\tau=2.5 \mu s$ ,  $I=100-200 \mu A$ ,  $S=0.1 \text{ mm}^2$ ,  $f=30-50 \text{ Gz}$ . The investigations were made at room and liquid nitrogen temperatures.

The investigation of pulse heat transfer and impurity diffusion in the heterostructure PS-silicon substrate we have carried out by numerical method of modelling. We have used three dot implicit numerical method for solving non-linear non-stationary diffusion equation, calculation of time evolution of temperature and concentration coordinate dependencies for heterostructure PS-silicon substrate.

## RESULTS AND DISCUSSION

PS optical properties were studied on the basis of ellipsometrical research. The relation of refractive indexes of PS pre-surface areas with the degree of porosity, which is in its turn determined by the parameters and duration of electrochemical etching of silicon, is shown in the Fig.1.

Refractive index decreases 2 times with the increase in porosity from 0 to 80%. The porosity was calculated from Lorentz-Lorenc equation [2]:

$$\frac{\tilde{n}_{por}^2 - 1}{\tilde{n}_{por}^2 + 2} = \frac{\tilde{n}_{Si}^2 - 1}{\tilde{n}_{Si}^2 + 2} (1 - p') + \frac{n_0^2 - 1}{n_0^2 + 2} p', \quad (1)$$

where:

$n_{Si}$ ,  $n_{por}$  – refractive indexes of silicium and porous silicon,

$n_0$  – refractive index of porous syrround,  $p'$ -porosity.

Optical parameters for this equation we obtained by numerical solving inverse problem of ellipsometry for two layers model (Table 1).

Thickness of porous silicon layer changed from 0.1 to 100 micrometers. Such a profound change of pre-surface areas can be attributed to the change of the composition of porous silicon surface films with different porosity in the process of electrochemical etching. On the basis of Auger spectroscopic experiments it has been determined that after a deep desorptional cleaning on the surface of (110) n-type plates there can be observed 43.5% of surface atoms of silicon combined with silicon diaoxide, 8.5% of not chemically active silicon atoms, 24.2% of oxygen atoms, 3% of nitrogen atoms and 20.8% of carbon atoms. The spalling of silicon in super high vacuum showed the following amounts: silicon – 36%, oxygen – 32% and carbon – 32%. It is completely different on PS surface. In our research, in the case of 40% porosity PS, surface layer contains 19% Si, 10% O, 71% C. The surface composition of 70% porosity silicon is as follows: Si – 18%, O – 10%, C – 72%. In PS Auger spectra, peaks of pure silicon, silicon oxides  $SiO_x$ , peaks of carbon and such elements as Cl, F, N, Fe can be observed. Presence of the mixture of oxides and silicon carbonates in the shape of surface film coatings as well as frectality of PS structure accounts for research on dielectrical PS properties. For this purpose TSDC method has been applied (Fig.2).

Table 1.

N	P, mg	$\Delta P$ , mg	t, min	$i$ , mA	d, $\mu$	$S, \bar{n}i^2$	$p$ , %	type of conductivity
1	68,269	0,99	5	20	6	0,51	29,7	n
2	74,694	1,151	5	30	8	0,6578	46,9	n
3	74,704	1,653	5	40	9	0,6463	61	n
4	51,876	0,325	1	10	4	0,3718	46,7	n
5	86,430	1,935	5	50	8	0,9161	57	n
6	74,162	1,554	10	20	7,5	0,665	66,8	n
7	96,840	1,252	20	10	8	0,675	23,3	n
8	68,245	0,189	5	5	3	0,64	21,1	p

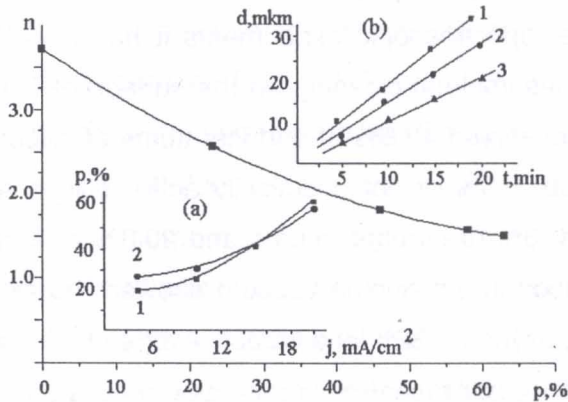


Figure 1. Refractive index dependence vs. porosity degree of PS:

Insert (a): PS porosity changes with increase in electrochemical etching current density, determined by gravimetric (1) and ellipsometric (2) methods.

Insert (b): Time electrochemical etching dependence of porous layer thickness for different etching current density: 1-30 mA/cm<sup>2</sup>, 2-20 mA/cm<sup>2</sup>, 3-10 mA/cm<sup>2</sup>.

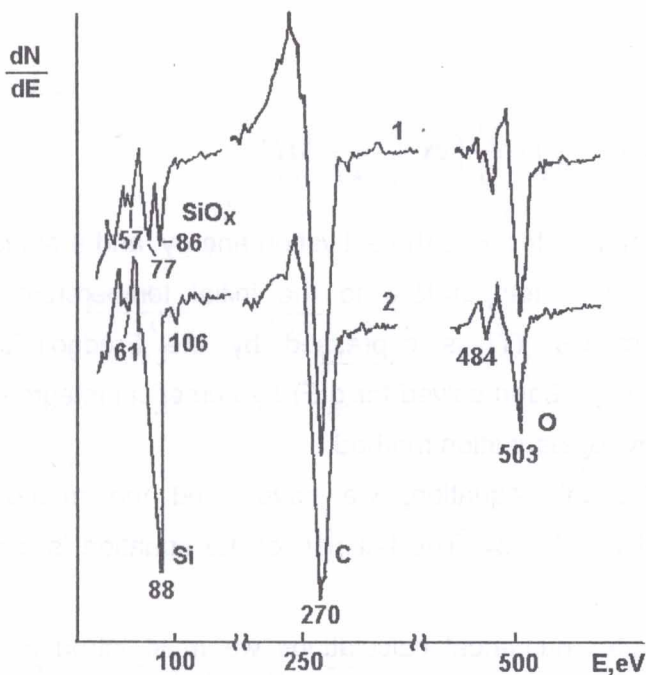


Figure 2. Silicon surfaces' Auger spectra: 1 – before electrochemical etching; 2 – after electrochemical etching (PS) with porosity  $p=40\%$ .

The typical TSDC spectra of the porous Si-Si substrate structures in the temperature range of 200-450 K are presented in Fig.3. Structures show quite evident maxima at the temperatures near 350-375 and 425-450 K. The TSDC spectra are not enough informative in identification of nature of the defects which are responsible for the electret state. That is why we have carried out the analysis of the energy distribution function  $g(E)$  of the involved in polarization defects. The phenomenological theory of TSD currents for disordered dielectrics with quasi-continuous energy distribution of the electrically active defects was used for this purpose. According to [2], the thermally stimulated discharge current  $j(T)$  can be written as follows:

$$J(T) = \int g(E)\xi(E,T)dE \quad (2)$$

where

$$\xi(E, T) = \omega \exp\left(-\frac{E}{kT}\right) - \frac{\omega}{\beta} \int_{T_0}^T \exp\left(-\frac{E}{kT'}\right) dT'$$

$\omega$  is the frequency factor,  $E$  is the activation energy, and  $\beta$  stands for the rate of increase in temperature to the initial temperature. For our experimental results  $j(T)$  is expressed by the Fredgolm's integral equation, which has been solved for  $g(E)$  by numerical integration based on the Tikhonov regularisation method.

To solve this equation, we have used the method of the regularisation by Tikhonov. The left part of the equation is a numerical file.

Thus, after numerical calculations we must introduce obtained energy activation distribution function for charged defects (ions) in porous silicon (Fig.3). There is a distribution function of fill electron states in energy gap by energy and frequency factor. From this curves we have seen exiting of thermoelectret condition in PS caused by redistribution of ions which are defects in PS. Obtained spectra were characterised not by one value of activation energy, but by a certain distribution.

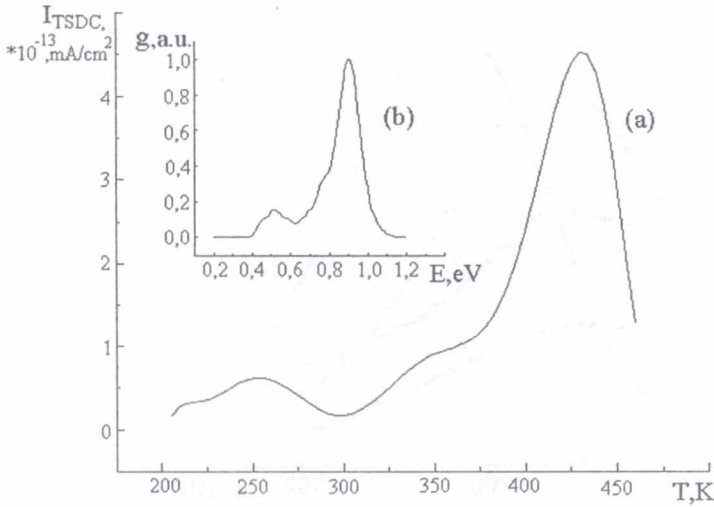


Figure 3. (a).The TSDC spectra of PS-Si heterostructure. Insert (b): The activation energy distribution functions of the defects in por-Si-Si heterostructure.

The intensive photoluminescence (PL) (which was visible at daylight) in p- and n-types of por-Si took place under the following conditions of exciting. PL properties of por-Si films were changed with electrochemical etching conditions, type and level of silicon substrates doping. Mathematical approximation of PL spectrum by Gauss curves allowed to ascertain that luminescence maximum of n-type porous Si specimens was at wavelength of about 660 nm, and intensity of peak depended on porosity values. In contrast, the maximum of luminiscence band of p-type was at  $\lambda$  almost equal to 667 nm. The intensity of light also depended on electrochemical etching conditions (Fig.4). Absolute value of PL intensity of p-type por-Si was higher than PL in n-type por-Si. PL intensity of n-type porous Si increased after additional chemical etching in pure HF, with the material porosity increase.



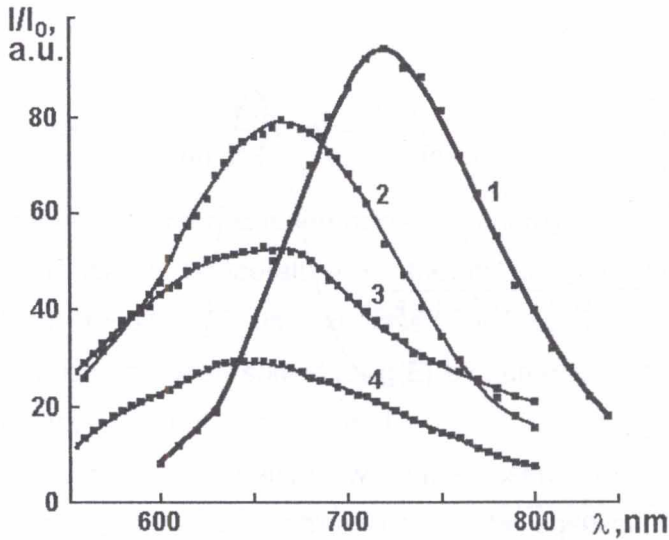


Figure 4. a) The photoluminescence spectra of por-Si under nitrogen (2, 3, 4) and argon (1) laser exciting at  $T=293$  K: 1-  $p=40\%$ , 2-  $p=40\%$ , 3-  $p=60\%$ , 4-  $p=44\%$  (1, 2- p-type Si, 3, 4- n-type Si).

We have studied the processes of polymetacrylic acid (PMA) polymer film precipitation from water solution on PS surface, considering the fact that chemical reactions on PS surface continue under atmospheric condition. Precipitation was conducted by placing PS samples into PMA water solution for 5-24 hours. PMA water solution with different molecular masses (10000-70000) and different ionization degrees (0-1.0) was used. Real medium speed of precipitation was  $0.8-1 \mu\text{m/h}$  for  $5-10 \mu\text{m}$  PMA film thickness.

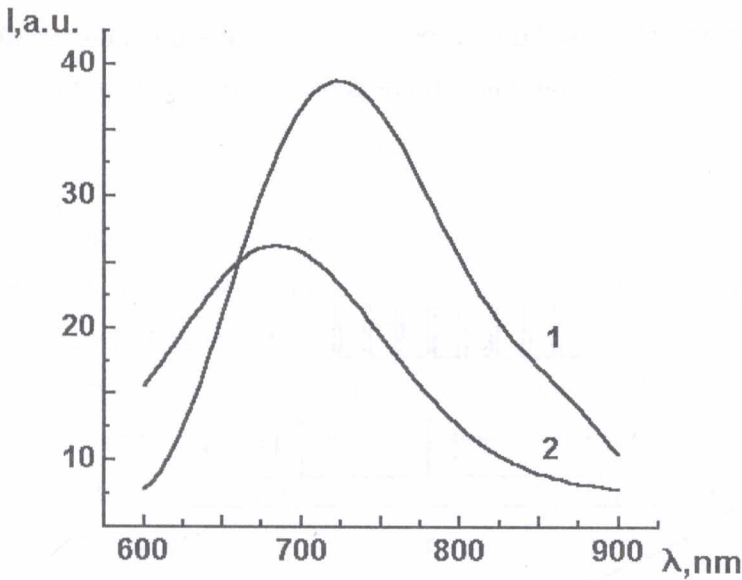


Figure 5. The photoluminescence spectra of PS with nature thin film coating (1) and with polymer film coating (2).

The obtained heterostructures of PS-PMA had photoluminescence properties. Photoluminescence spectrum of the PS was transformed due to interaction between PMA and the PS surface. Photoluminescence curves had gaussian shape with one wide maximum at a room temperature, which was shifted by 70-80 nm towards short wave band of the spectrum, comparing with PS spectrum without polymer film. The maximum of luminescence was located at about 600-625 nm due to the ionization degree. Luminescence at the maximum decreased 2-2.5 times with the increase in intensity (Fig.5).

EL with wide band in the wavelength range of 500-900 nm was observed for various regimes under direct PS shift. Under inverse PS shift, EL intensity approximated zero. Integrated PS EL, which was registered by PEM-62 photoelectronic multiplier, decreased after switching on the injection direct current. That was especially characteristic

for p-type PS samples, when the integrated intensity decreased twice during 1 minute. We investigated the influence of the character of pulsed excitation regime on EL intensity and degradation (Fig.6).

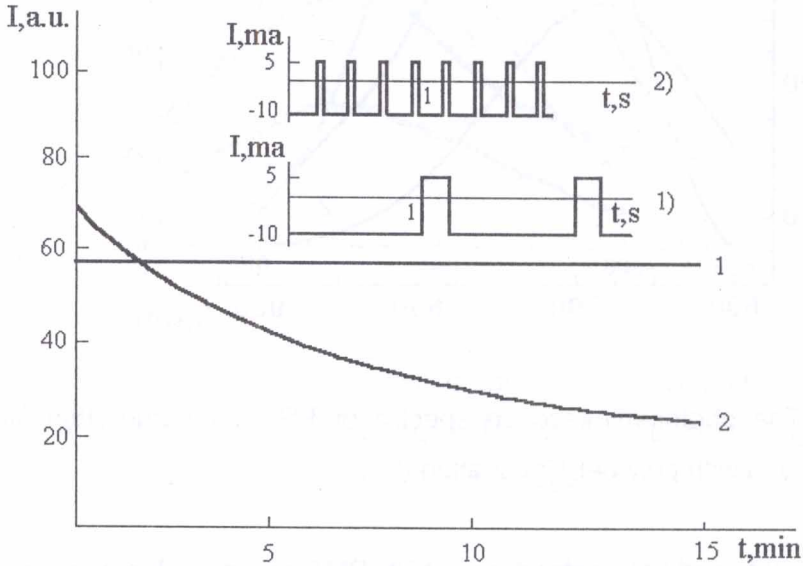


Figure 6. Time dependence of maximum EL intensity decay: 1-a)-type injection current; 2-b)-type injection current.

For n-type samples, EL PS intensity was by an order higher than for those of p-type, and it was stable during the time of measurements (30 minutes). EL was excited by periodic direct and inverse pulses of 1 and 0,2 second duration, respectively, and with -10 and +5 mA amplitude. A peculiar feature here is full reproduction of EL spectra after the fifth measurement. That is, in this excitation regime no irreversible changes were observed.

EL bandwidth did not change when EL was excited by short duration pulses (direct pulse of duration – 0,2 sec. and inverse – 0,05 sec.) with the previous values of current. Nevertheless, EL intensity in

maximum increased by 25% and it did not change for 30 minutes during 5 consecutive measurements, but decreased exponentially by 3-5 times as compared with the initial one. EL degradation was irreversible. EL restoration was possible only after electrochemical etching of the sample in HF (30 minutes), what probably resulted in dissolution of the oxide film on PS surface. It should however be mentioned that the intensity of renewed EL was 5-10 times less than the initial one, what may be explained by reduction of PS layer thickness. Spectral dependence of PS EL decay rate was investigated by us in the inverse changes regime, that is, in the regime of long duration pulses (direct pulse 1 sec., inverse pulse 0,2 sec.). EL decay rate was different when the inverse pulse was sent with different wavelengths. Moreover, intensity decay within the same testing time was greater for EL short wavelength part of the spectrum. That is, there are the groups of EL in PS centres which are characterized by sharp decay kinetics: short wavelength groups by faster kinetics, and long wavelength by slower kinetics.

We have also investigated cathodoluminescence (CL) from PS. Two dominant CL bands with maximum in visible (at 550-570 nm) and ultraviolet (360-380 nm) regions were observed (Fig.7). The intensity of short wave band was several times greater, but decrease rate was very high comparing with long wave decrease rate.

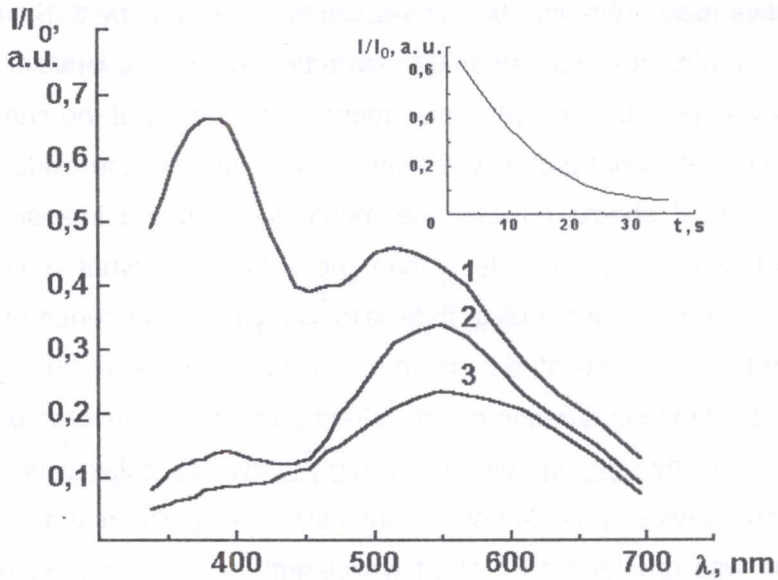


Figure 7. CL PS spectrum at 77 K (1,2) and 300 K (3) at initial time moment (1,3) and after 20 min.(2). Insert - CL time intensity decay at  $\lambda_{\max}$ .

CL blue band confirms the existence of dielectric coating on quantum wires surface ( $\epsilon_g \approx 3.1$  eV). Long wave CL peak shifts into short wave region with comparatively the same bands of PL and EL ( $\epsilon_g \approx 2.4$  eV). This may be connected with different depth of exciting PL, EL, CL and absorption of radiation by porous silicon.

Decrease in kinetics of these luminescence types was different: PL was stable during investigation time ( $\sim 1$  h). Decreasing times for CL and EL were 15-20 min and 10-15 min. So the photo-, electro- and cathodoluminescence in porous silicon have strongly different nature.

Electron Paramagnetic Resonance (EPR) investigations of the highly pure unannealed samples of commercial silicon have shown that in all samples no EPR spectrum was observed at temperatures of 300 and 77 K. The same samples of silicon in the porous state are characterized by a weak EPR signal of approximately symmetric lineshape with  $g_{\text{eff}} =$

$2.0055 \pm 0.0005$  and peak-to-peak derivative linewidth -  $\Delta H_{pp} \approx 9,5$  G (Fig.8).

This EPR signal is similar to the signals registered in the cleaved in vacuum and powdered in air Si single crystals and interpreted as a signal of the broken surface bonds. Annealing of the porous silicon in vacuum ( $P \approx 10^{-1}$  Pa) at  $T = 723$  K during 1 hour leads to a significant increase in the EPR signal of surface broken bonds and causes appearing of the new EPR line ( $g_{eff} \approx 2.0015$ ) which arises in the low-field asymmetric shoulders of the linewidth  $g_{eff} \approx 2.0055$ . It should be noted that the EPR signal with  $g_{eff} \approx 2.0055$  in porous silicon was observed also in [6] after heating in vacuum.

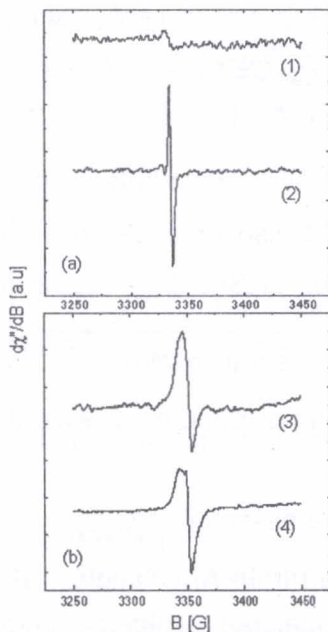


Figure 8. EPR spectra of the porous silicon unannealed (a) and annealed in vacuum ( $P=10^{-1}$  Pa) at  $T=623$  K during 1 hour (b). The upper spectra (1, 3) in (a) and (b) are recorded at  $T=300$  K; the lower spectra (2, 4) are the same spectra recorded simultaneously with DPPH marker.

The PS TSEE spectra have been studied depending on: exposition time of the samples in laboratory atmosphere after formation of porous structure; exposure in vacuum; porosity degree and also on the dose of electron irradiation. Primarily, it has been reported [6] about TSEE spectra of por-Si samples ( $p \approx 30\%$  porosity) exposed to laboratory atmosphere after electrochemical etching (exposition times from several hours up to several days) which have an intensive maxima at  $380\div 390$  K,  $440\div 450$  K and  $520\div 540$  K temperature range during the first heating. (Fig.9) shows TSEE spectra of PS ( $p \approx 80\%$  porosity) previously exposed in vacuum chamber ( $P \approx 10^{-1}$  Pa) during a prolonged time (2+3 months). TSEE spectrum reveals only one intensive  $350\div 475$  K maximum at the first heating and, as in the previous case, maxima are almost absent during repeated heating. Therefore, it was concluded that maxima at TSEE spectra at the first heating basically resulted from a partial desorption of  $\text{CO}_x^-$ ,  $\text{O}_x^-$ ,  $\text{OH}^-$  adsorbates weakly bounded with the developed PS surface, and also from electron emission during certain physical-chemical processes in  $\text{Si}_y\text{O}_x\text{C}_{1-x-y}$  adsorbates mixtures thin film coatings. The value of integral exosum  $\Sigma = \int_{295\text{K}}^{650\text{K}} I_{\text{TSEE}}(T) dT$  tends to increase with an increase in por-Si porosity, what is the result of effective emission area increase.

The existence of the essential  $\text{Si}_y\text{O}_x\text{C}_{1-x-y}$  coatings on the surface of por-Si is confirmed, apart from AES studies, also by results of TSEE studies of electron beam irradiated samples previously thermocycled and annealed in the vacuum. (Fig.9) shows TSEE spectra of por-Si after various doses of irradiation by electron beam. Two intensive maxima at  $315\div 325$  K and  $350\div 400$  K appear in the TSEE spectra, proving the availability of at least two types of exoemission centres. Calculated activation energies and frequency factors for processes that occur at the

first and the second TSEE peak are 0.90 eV;  $5.0 \cdot 10^{12} \text{ s}^{-1}$  and 1.11 eV;  $5.88 \cdot 10^{12} \text{ s}^{-1}$ , respectively. It is well known that TSEE from clean Si surfaces without oxides' coatings, which are dielectric (for example  $\text{Si}_y\text{O}_x\text{C}_{1-x-y}$ ), doesn't reveal at the first heating as well as after electron irradiation. At the same time TSEE spectra with intensive exoemission peaks are typical for  $\text{SiO}_x$  compounds.

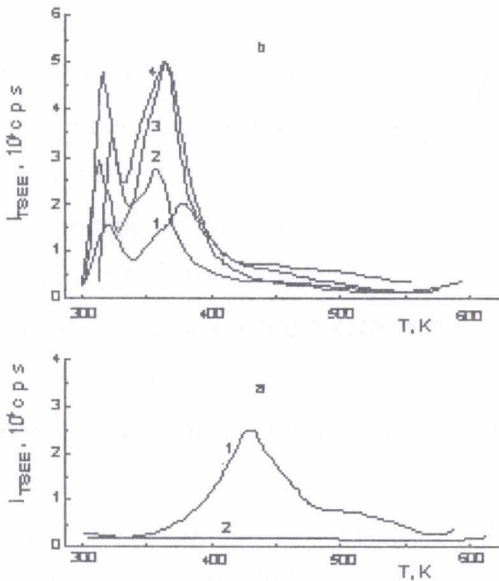


Figure 9. Thermostimulated exoelectron emission (TSEE) spectra of porous Si ( $p=80\%$  porosity):

- a) 1 - first heating; 2 - second heating;  
 b) after previous heating and next electron beam irradiation ( $E=3 \text{ keV}$ ,  $j=700 \text{ A/m}^2$ ); during time: 1 - 2 min; 2 - 8 min; 3 - 45 min; 4 - 240 min.

- It should be noted that problem of amorphous, glassy or polycrystalline origin of thin film oxide layer on newly created real Si surfaces is still controversial. Therefore, the exoemission probability of electrons and weakly bounded components (as negative charged ions) from thin film coatings during the first heating increases in consequence



of possible reconstruction while heating of  $a\text{-Si}_y\text{O}_x\text{C}_{1-x-y}$  thin films structure and phase transformations. This leads to considerable decrease in exoemission activity up to its disappearance during repeated heating of por-Si and obtaining the phase-thermodynamic equilibrium in  $a\text{-Si}_y\text{O}_x\text{C}_{1-x-y}$  coatings.

We have investigated theoretically the temperature fields in porous silicon-Si heterostructures(PS-Si) under pulse-periodic laser irradiation, using method of numerical modelling. Effective thermal conductivity was calculated basing on the two layer model. We have shown that heterogeneous temperature distribution has taken place, and its maximum has penetrated into the depth of the crystal in the course of time (Fig.10). We have shown by calculation that the surface heterostructure temperature increase with time has had almost linear character . It has reached maximum value at the final moment of pulse duration. Next, temperature has decreased exponentially to the level which has been determined by time interval between laser pulses.

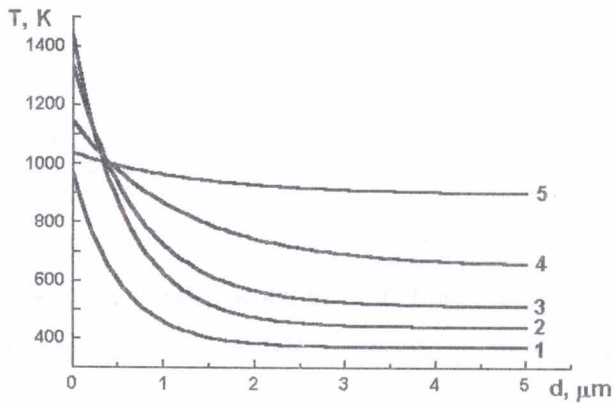


Figure 10. Temperature distance distributions calculation in heterostructure PS-silicon substrate under laser pulse irradiation: 1 -  $0.25\tau$ , 2 -  $0.5\tau$ , 3 -  $0.75\tau$ , 4 -  $\tau$ , 5 -  $2\tau$ .

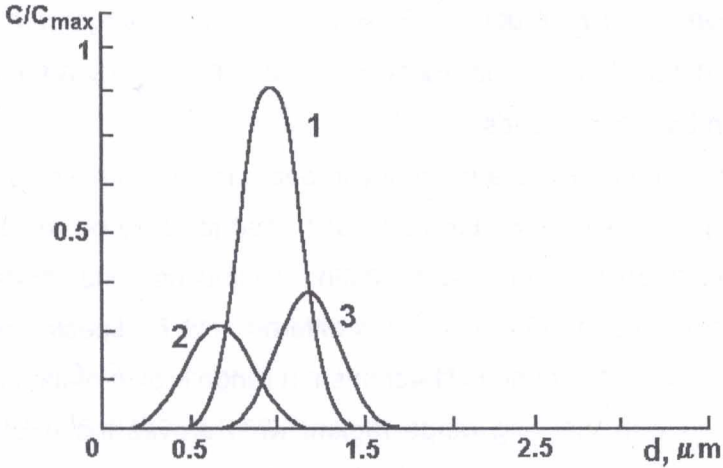


Figure 11. Impurity concentration profiles changing in PS under laser pulse irradiation:

1- initial distribution, 2,3-time evolution of initial profile.

Using implicit numerical method, we have investigated redistribution process of charged impurities in PS under laser pulse irradiation. In diffusion mass transfer, conditions of the initial distribution have changed: depending on impurity type and its concentration level, it has drifted and accumulated the impurities to normal to irradiated surface. This phenomenon is connected with the influence of inside electrical and thermomechanical fields under heterogeneous heating. We have calculated ion-implanted impurity evolution in PS for different pulse heating conditions. Obtained distribution has „anomalous” character: initial distribution not only blurs but its maximum is moved into PS depth (Fig.11).

## CONCLUSIONS

All specimens have wide band of PL with maximum in range from 650 nm to 760 nm. Intensity of n-type por-Si specimens PL is by 5÷6 times lower than from p-type por-Si ones.

Thus, PS EL intensity has a tendency to decrease when passing through direct and pulsed injection current. These changes may be reversible or irreversible, depending on the excitation conditions. The character of luminescence fatigue in both cases is different. PS EL spectral decay in the inverse changes regime is faster in short range region of the spectrum as compared with the long range region, what proves the existence of different types of kinetic radiation centres in PS.

It has been established that phase transformations, which are accompanied by emission of negative charged particles, occur in a  $\text{Si}_y\text{O}_x\text{C}_{1-x-y}$  thin film coatings, existing on the surfaces of por-Si. The dielectric amorphous thin films  $\text{a-Si}_y\text{O}_x\text{C}_{1-x-y}$  oxygen-carbon coatings with energy gap value equal to 3.4÷3.5 eV and high effective area might play a significant role in PL of por-Si.

The analysis of Auger spectra of porous silicon shows that after the electrochemical etching of silicon, the phase containing silicon or  $\text{SiH}_y$ , oxygen and carbon is registered convincingly .

Simultaneously it has been shown that after the electrochemical etching, the intensive photo- and electroluminescence of silicon is observed. These samples of porous silicon reveal faint paramagnetic properties. However, after thermal treatment in vacuum at 670÷720 K, the complete quenching of luminescence is observed and EPR signal appears for above mentioned samples.

The EPR spectrum was similar to the spectrum of broken Si bonds in the volume of amorphous Si:H or dangling Si bonds on the surface of the atomically clean crystalline silicon.

The intensive maximum, originated from the presence of adsorbates on the surface of porous silicon, is typical for TSEE spectra only at the first heating and it is almost absent during the repeated heatings. Further peaks at TSEE spectra appear only after electron beam irradiation of porous Si.

Consequently it can be concluded that: the surface of porous silicon is non homogenous, containing fragments of Si or  $\text{SiH}_y$  and also thin dielectric coatings of Si-O-C system;

apart from Si-O-C clusters on the surface, the  $\text{SiH}_y$  coatings play a significant role in the light emission of porous silicon.

PS refractive index increases more than three times, when porosity is decreased from 0 to 70 %. This may be connected with a modification of changing of air volume in PS and changing of PS surface composition.

We have shown the presence of both fragments of  $\text{SiO}_x\text{C}_y$  and pure Si (or  $\text{SiH}_y$ ) on the surface of PS. Thus, PS has dielectric properties such as TSD current and UV-cathodoluminescence. But such properties, as visible photoluminescence, excited by  $\text{N}_2(0.875 \mu\text{m})$  and  $\text{Ar}(0.48 \mu\text{m})$ , are rather connected with the presence of  $\text{SiH}_y$ -clusters on the PS surface. In agreement with this hypothesis, an EPR spectrum of PS annealed and unannealed in vacuum, and TSSE of PS are obtained. We have shown the existence of broken Si bonds in the amorphous Si:H, dangling Si bonds on the surface of crystalline Si and  $\text{OH}^-$  adsorbates in PS surface coating. The possibility of precipitation of PMA film on PS surface have been used to isolate PS from external and atmospheric influences. Thus, basing on our investigations we have ascertained that the surface of porous silicon is not homogenous, and contains fragments Si or  $\text{SiH}_y$  and also thin dielectric coating of  $\text{SiO}_x\text{C}_y$ .

Moreover SiOC clusters on the surface and  $\text{SiH}_y$  coatings play a significant role in the light emission of porous silicon. The intensive PL, EL and CL of PS observed in all samples have wide band of PL with

maximum in the range from 650 nm to 750 nm. Por-Si LE intensity has a tendency to decrease when passing direct and pulsed injection current through the electrochemical cell. This spectral decay is connected with the depolarisation process in PS.

## REFERENCES

1. L.T. Canham. Appl.Phys.Lett. 57, 1046 (1990)
2. M. Born, E. Wolf. Principles of optics. Pergamon Press 719 (1968)
3. L.Monastyrskii, T.Lesiv, I.Olenych. Thin Solid Films (1999).
4. M.F. Chung, D. Haneman. J. Appl. Phys. 37, 1879 (1966)
5. D. Haneman. Phys. Rev. 170, 705 (1968)
6. P.K. Kashkarov, E.A. Konstantinova, V.Yu. Timoshenko. Phys. and Tech. of Semicond. 30 1479 (1996)
7. P.V. Galiy, T.I. Lesiv, L.S. Monastyrskii, T.M. Nenchuk, I.B. Olenych. Thin Solid Films. 318,113 (1998)